

Self-diffusion in bidisperse systems of magnetic nanoparticlesAlla B. Dobroserdova **Ural Mathematical Centre, Ural Federal University, Named after the First President of Russia B. N. Yeltsin, Ekaterinburg 620002, Russia*Sofia S. Kantorovich †*University of Vienna, Faculty of Physics, Kolingasse 14-16, 1090, Vienna, Austria,
and Ural Federal University Named after the First President of Russia B. N. Yeltsin, Ekaterinburg 620002, Russia;
and Research Platform MMM, University of Vienna, Oskar-Morgenstern-Platz 1, 1090, Vienna, Austria*

(Received 30 September 2020; accepted 9 December 2020; published 27 January 2021)

In the present paper, we study the self-diffusion of aggregating magnetic particles in bidisperse ferrofluids. We employ density functional theory (DFT) and coarse-grained molecular dynamics (MD) simulations to investigate the impact of granulometric composition of the system on the cluster self-diffusion. We find that the presence of small particles leads to the overall increase of the self-diffusion rate of clusters due the change in cluster size and composition.

DOI: [10.1103/PhysRevE.103.012612](https://doi.org/10.1103/PhysRevE.103.012612)**I. INTRODUCTION**

The terms magnetic fluids, ferrofluids, or magnetic colloids are used to address the systems that consist of single-domain magnetic nanoparticles suspended in a carrier liquid [1–3]. In such systems, magnetic nanoparticles can be well approximated by point dipoles, whose directions are determined by the particles' internal anisotropy and by the external magnetic field direction, if the latter is applied. In the past three decades, thanks to their ability to interact with an external magnetic field and keep the liquid state at the same time, ferrofluids have found multiple applications in technology [4] and medicine, such as drug targeting, magnetic resonance imaging, and magnetic hyperthermia [5–11]. Important parts of medical applications rely on knowledge of the diffusive properties of magnetic particles in liquid carriers in the absence of an applied field. Thus, the main aim of this paper is to study the impact of interparticle interactions and particle polydispersity on the self-diffusion coefficient in a system of magnetic dipolar particles. In other words, we will study the equilibrium condition in which the average particle's mobility depends on the particle being a member of various ferroparticle aggregates and can be considered constant in time due to the steady cluster size distribution. In such systems, in contrast to those described, for example, by Licinio *et al.* [12], the average cluster size is constant in time.

The self-diffusion coefficient $D(t)$ is a proportionality factor between the mean squared displacement $\langle x^2(t) \rangle$ and time t ,

$$\langle x^2(t) \rangle = \frac{1}{dN} \sum_{i=1}^N \sum_{j=1}^d [x_j^i(t)]^2 = 2D(t)t, \quad (1)$$

where $x_j^i(t)$ is the j th coordinate of the d -dimensional space of the i th particle in a time moment t , N is the total number of particles in the system, and the operation $\langle \cdot \rangle$ means the averaging over all coordinates of all particles in the system. In this work, we investigate self-diffusion of permanently magnetized ferromagnetic nanoparticles in bulk, $d = 3$, and in quasi-two-dimensional (quasi-2D) layers, where the translations are in one plane but the rotations are not constrained, $d = 2$.

There are several works where the diffusive behavior of magnetic nanoparticles was investigated [13–23]. The main differences of this paper from the previous studies is that here we propose a method to analytically calculate $D(t)$, taking into account self-assembly and polydispersity of magnetic particles as well as the spatial constraints imposed on the ferrofluid sample in one model. This analytical model is verified using coarse-grained hydrodynamics-free MD simulations. The choice to ignore the hydrodynamics in the simulations was dictated by the necessity to first thoroughly understand the effects of interparticle magnetic interactions and system dimension on the self-diffusion in a thermodynamic equilibrium.

The paper is organized as follows. First, in Sec. II, the analytical approach based on the DFT is explained; next, in Sec. III, the simulations performed to verify the theoretical models are described. The results are provided in Sec. IV and the brief summary and outlook are in Sec. V.

II. THEORETICAL MODEL

Real magnetic fluids are inevitably polydisperse and might have mixed relaxation mechanisms: Néel or Brownian [1]. When developing a theoretical model of the self-diffusion, however, it is neither possible to accurately allow for a broad particle-size distribution nor possible to describe various magnetization mechanisms. In this work, we consider a bidisperse

*Alla.dobroserdova@urfu.ru

†Sofia.kantorovich@univie.ac.at

approximation to polydispersity. It means that the model system contains particles of two distinct sizes. The choice of a bidisperse system is justified by the previous works [24–27], showing that the impact of polydispersity can be already seen in such a simplified approach [28]. As for the particle magnetism, we focus on ferromagnetic single domain particle whose behavior can be successfully modeled by point dipoles [25].

Along with particle polydispersity, the sample geometry can also affect structural properties of magnetic fluids. In order to include the influence of the sample dimension in the model, we investigate a model bidisperse magnetic fluid in two different geometries. The first case is a fully three-dimensional system, while in the second case, nanoparticle centers are constrained to move in one plane, but the rotations are free. The second geometry is usually addressed as a quasi-two-dimensional layer [29–41].

Below, for simplicity, we will discriminate between small and large particles when describing the theoretical approach. The main interaction between magnetic nanoparticles is the non-central and long-range magnetic dipole-dipole one [42]:

$$U_{dd}(i, j) = \frac{\mu_0}{4\pi} \left(\frac{\langle \vec{m}_i, \vec{m}_j \rangle}{|\vec{r}_{ij}|^3} - \frac{3\langle \vec{m}_i, \vec{r}_{ij} \rangle \langle \vec{m}_j, \vec{r}_{ij} \rangle}{|\vec{r}_{ij}|^5} \right), \quad (2)$$

where \vec{m}_i and \vec{m}_j are the magnetic moments of i th and j th magnetic particles, respectively, \vec{r}_{ij} is the vector connecting the centers of i th and j th particles, and $\mu_0 = 4\pi \times 10^{-7}$ H/m is the magnetic permeability of vacuum.

We can characterize this interaction using the parameter λ_{ij} , which is the ratio of the magnetic energy of two particles, i and j , in close contact with dipoles aligned head to tail to the thermal one, $k_B T$, with k_B denoting the Boltzmann constant:

$$\lambda_{ij} = \frac{\mu_0 |\vec{m}_i| |\vec{m}_j|}{4\pi k_B T \sigma_{ij}^3}, \quad i, j \in \{s, l\},$$

$$\sigma_{ij} = \frac{\sigma_i + \sigma_j}{2}, \quad i, j \in \{s, l\},$$

where indices s and l stand for small and large magnetic particles, respectively, and σ_{ij} is the distance between two touching particles with diameters σ_i and σ_j .

A short-range repulsion between particles is described by the Weeks-Chandler-Andersen (WCA) potential [43], which also well known as the truncated and shifted version of the Lennard-Jones potential [44]:

$$U_{\text{WCA}}(i, j) = \begin{cases} 4\varepsilon \left[\left(\frac{\sigma_{ij}}{|\vec{r}_{ij}|} \right)^{12} - \left(\frac{\sigma_{ij}}{|\vec{r}_{ij}|} \right)^6 \right] + \varepsilon, & |\vec{r}_{ij}| \leq r_{ij}^c, \\ 0, & |\vec{r}_{ij}| > r_{ij}^c, \end{cases} \quad (3)$$

where ε is the potential well depth of the Lennard-Jones interaction. WCA potential is purely repulsive and the cutoff $r_{ij}^c = 2^{1/6} \sigma_{ij}$ corresponds to a distance where it goes to zero.

If magnetic forces are strong enough in comparison to thermal fluctuations, magnetic particles form clusters, whose main topology is a chain in bulk, whereas in quasi-2D layers along with chains, rings can be formed [30–32]. If the temperature decreases even more, rings, branched structures, and percolating networks are observed [45–48], but this regime goes beyond the scope of this study.

A. Three-dimensional bidisperse ferrocolloids

The system is considered to be in a thermodynamic equilibrium; therefore, the free energy density functional has been chosen as the basis for the proposed theoretical approach [49] that is equivalent to the Wertheim's theory actively used to describe the equilibrium self-assembly in patchy colloids. See Ref. [50] and references therein. Extending the work of Ref. [49], where the free energy was calculated in the simplest monodisperse approach in the limit of strong aggregation, the expression for the free energy of a bidisperse ferrocolloid in bulk can be written as [25]

$$F_{3D,bi} = k_B T \sum_{n+m=1}^{\infty} \sum_{i=I}^{IV} K(i, n, m) g(i, n, m) \times \left[\ln \frac{g(i, n, m) v(i, n, m)}{e} - \ln Q(i, n, m) \right],$$

$$v(i, n, m) = v_s^{-\alpha_i} v_{sl}^{m-\beta_i} v_l^{n-\gamma_i},$$

$$v_{ij} = \frac{\pi}{6} \sigma_{ij}^3, \quad i, j \in \{s, l\}, \quad v_{ss} = v_s, \quad v_{ll} = v_l, \quad (4)$$

where $g(i, n, m)$ is a number concentration of chains from the i th topological class composed of n large and m small particles; $v(i, n, m)$ is a normalizing volume for a bidisperse three-dimensional ferrofluid; α_i , β_i , and γ_i are the numbers of small-small, small-large, and large-large particle contacts in chains, respectively; $K(i, n, m)$ is a combinatorial factor equal to a number of entropically distinguishable chains in the i th topological class with n large and m small particles; and $Q(i, n, m)$ is a partition function for chains of i th topological class with n large and m small particles [25]. Notice that the first part of the sum is the entropy of an ideal gas of various clusters, whereas the second part contains energetic contributions.

The functional (4) is minimized with respect to $g(i, n, m)$ using the Lagrange multiplier method under mass balance conditions, which mean a constant amount of particles in the system:

$$\frac{\varphi_s}{v_s} = \sum_{n+m=1}^{\infty} \sum_{i=I}^{IV} K(i, n, m) g(i, n, m) n, \quad (5)$$

$$\frac{\varphi_l}{v_l} = \sum_{n+m=1}^{\infty} \sum_{i=I}^{IV} K(i, n, m) g(i, n, m) m, \quad (6)$$

where φ_s and φ_l are volume fractions of small and large particles, respectively.

After the minimization, all equilibrium concentrations $g(i, n, m)$ for chains are obtained.

The microstructure of a bidisperse system in bulk was shown to mainly consist of four topological chain classes: chains consisting of large particles only (class I), chains of large particles with a small one at the end of chains (class II), chains of large particles with two small ones at the ends of chains (class III), and chains of small particles (class IV). Earlier, we ignored the possibility of small particles to form chains, as such clusters were insignificant for the magnetization description works [25,51]; here, instead, allowing for them is essential to calculate accurately the self-diffusion (for

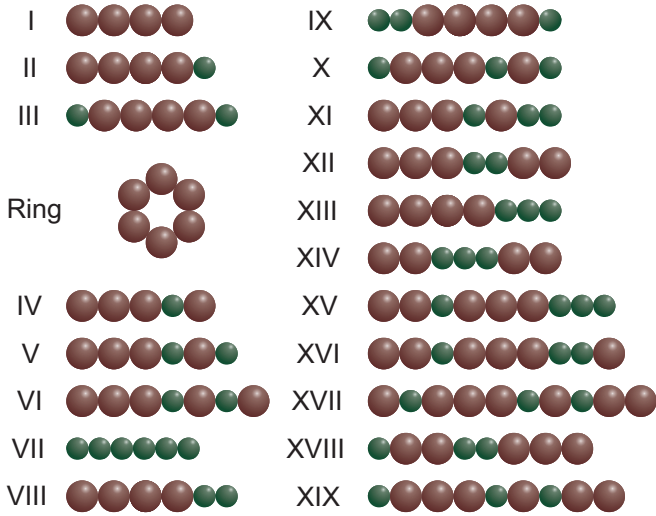


FIG. 1. The microstructure of bidisperse thin films of magnetic fluids.

details, see Sec. IV). The topology of the clusters in bulk corresponds to structures I, II, III, and VII in Fig. 1.

In order to calculate the self-diffusion coefficient in the system, we need to calculate the self-diffusion for each structural element individually. Considering the fact that we are focused on the parameter regime where formed chains are short, we approximate them by ellipsoids with a major semiaxis a and two minor ones b . We can write the average mobility coefficient for ellipsoids:

$$\langle M_{3D}^{rr}(k) \rangle = \left[\frac{G_a^{rr}(k) + 2G_b^{rr}(k)}{3} \right]^{-1}, \quad (7)$$

$$G_a^{rr}(k) = \frac{8}{3} \left[\frac{2k}{1-k^2} + \frac{2k^2-1}{(k^2-1)^{3/2}} \ln \frac{k+\sqrt{k^2-1}}{k-\sqrt{k^2-1}} \right]^{-1}, \quad (8)$$

$$G_b^{rr}(k) = \frac{8}{3} \left[\frac{k}{k^2-1} + \frac{2k^2-3}{(k^2-1)^{3/2}} \ln(k+\sqrt{k^2-1}) \right]^{-1}, \quad (9)$$

where $k = \frac{a}{b}$ is the aspect ratio of an ellipsoid, $G_a^{rr}(k)$ and $G_b^{rr}(k)$ are geometric factors which characterize the amount of a deviation of the ellipsoid from a sphere. The factors $G_a^{rr}(k)$ and $G_b^{rr}(k)$ were obtained by Perrin [52] and used to calculate the diffusion coefficients for ellipsoids in several works for both three-dimensional and quasi-two-dimensional geometries [53–57].

With equilibrium concentrations $g(i, n, m)$ and the mobility coefficients $\langle M_{3D}^{rr}(k) \rangle$ (7) for ellipsoids approximating the chains at hand, we can calculate the translational self-diffusion coefficient in a bidisperse ferrofluid in bulk as follows:

$$D_{3D,bi}^{rr} = \left(\frac{\varphi_s}{v_s} + \frac{\varphi_l}{v_l} \right)^{-1} \times \sum_{n+m=1}^{\infty} \left[\frac{\sigma_l}{\sigma_s} \sum_{i=1}^{III} K(i, n, m) g(i, n, m) \langle M_{3D}^{rr}(k_i(n, m)) \rangle + g(IV, 0, m) \right]. \quad (10)$$

Note that the coefficient $D_{3D,bi}^{rr}$ (10) is normalized by the self-diffusion coefficient of a small magnetic particle.

B. Quasi-two-dimensional bidisperse ferrofluids

Quasi-two-dimensional geometry assumes that particle centers move in one plane and magnetic moments rotate freely. There are some differences in free energy description between three- and quasi-two-dimensional geometries. The main one is that entropic changes due to geometrical constraints lead to much more versatile cluster topologies in comparison to bulk. Four main classes considered above for bulk are not enough to obtain the right results in thin films [58,59]. Not only are new chain classes to be taken into account, but also the rings formed by large particles are to be considered [29–32]. Thus, the accurate description of clusters formed in bidisperse monolayers requires 19 chain classes and rings of large particles as shown in Fig. 1 [58].

In order to properly allow for the entropic changes stemming from quasi-2D geometry, one needs to modify the free energy functional (4). This can be done by adding the excluded area $S_{\text{excl},bi}$ interactions [29,58]. Excluded area around chains and rings is the area where the centers of other particles cannot be. The details of the excluded area calculation can be found in the work [58]. In order to write the free energy density functional for a bidisperse quasi-two-dimensional magnetic fluid, we introduce the function, $S_{\text{av},bi}$, that shows the area available for particle centers,

$$S_{\text{av},bi} = S - S_{\text{excl},bi} = S \cdot \tilde{S}_{\text{av},bi},$$

with S denoting the total area of a monolayer.

The free energy density functional for a quasi-2D layer of a bidisperse ferrocolloid can be written as [58]

$$F_{q2D,bi} = k_B T \sum_{n+m=1}^{\infty} \sum_{i=1}^{XIX} K(i, n, m) g(i, n, m) \times \left[\ln \frac{g(i, n, m) s_{\text{chain}}(i, n, m)}{e \tilde{S}_{\text{av},bi}} - \ln Q(i, n, m) \right] + k_B T \sum_{n=5}^{\infty} f(n) \left[\ln \frac{f(n) s_{\text{ring}}}{e \tilde{S}_{\text{av},bi}} - \ln W(n) \right],$$

$$s_{\text{chain}}(i, n, m) = s_s^{-\alpha_i} s_{sl}^{m-\beta_i} s_l^{n-\gamma_i}, \quad s_{\text{ring}} = s_l,$$

$$s_{ij} = \frac{\pi}{4} \sigma_{ij}^2, \quad i, j \in \{s, l\}, \quad s_{ss} = s_s, \quad s_{ll} = s_l, \quad (11)$$

where $f(n)$ is a number concentration for rings consisting of n large particles ($n \geq 5$), $W(n)$ is a partition function for rings of n large particles, and $s_{\text{chain}}(i, n, m)$ and s_{ring} are normalizing areas for terms corresponding to chains and rings, respectively. Here, the entropic part of the functional contains the first-order correction for intercluster interactions through the excluded area factors. Magnetic intercluster interactions are still not considered. This sets the limitations on the particle area fraction and the magnetic interaction strength as will be clarified below when comparing analytical predictions to the results of the simulations.

The functional (11) is minimized similarly to the bulk case with respect to chain and ring concentrations by the Lagrange multiplier method under mass balance conditions which can be written in the thin film as follows:

$$\frac{\rho_s}{s_s} = \sum_{n+m=1}^{\infty} \sum_{i=1}^{XIX} K(i, n, m)g(i, n, m)m, \quad (12)$$

$$\frac{\rho_l}{s_l} = \sum_{n+m=1}^{\infty} \sum_{i=1}^{XIX} K(i, n, m)g(i, n, m)n + \sum_{n=5}^{\infty} f(n)n, \quad (13)$$

where ρ_s and ρ_l are area fractions of small and large particles, respectively. After the minimization of the functional (11), we know equilibrium concentrations $g(i, n, m)$ for chains and $f(n)$ for rings.

In order to approximate chains in the monolayers, we use ellipsoids just as we did in a three-dimensional case (see Sec. II A). The average mobility for chains in quasi-2D systems has a slightly different form in contrast to (7) due to the geometrical constraints:

$$\langle M_{q2D, ch}^{tr}(k) \rangle = \left(\frac{G_a^{tr}(k) + G_b^{tr}(k)}{2} \right)^{-1}. \quad (14)$$

For an approximation of a ring, we have chosen a torus with the major radius c and minor one h :

$$c = \frac{2\sigma_l}{\sqrt{2(1 - \cos \frac{2\pi}{n})}}, \quad h = \frac{\sigma_l}{2}, \quad \xi = \frac{h}{c},$$

where ξ is the ratio of a major radius to minor one.

The geometric factor for a torus, analogous to those for ellipsoids given by Eqs. (8) and (9), has the following form:

$$F_a^{tr}(\xi) = \frac{4}{3}b \frac{Z(\xi) - 3}{(Z(\xi) - \frac{1}{2})(Z(\xi) - 2) - 2}, \quad Z(\xi) = \ln \frac{8}{\xi}.$$

Here, the translational motion can only happen in two directions along the major radius. The factor $F_a^{tr}(\xi)$ was obtained by Johnson and Wu [60] and was used to calculate the diffusion coefficients for a torus by Thaokar [61].

The average mobility for the torus has the following form:

$$\langle M_{q2D, r}^{tr}(\xi) \rangle = F_a^{tr}(\xi). \quad (15)$$

Using obtained equilibrium concentrations $g(i, n, m)$ for chains and $f(n)$ for rings and the average mobility coefficients $\langle M_{q2D, ch}^{tr}(k) \rangle$ and $\langle M_{q2D, r}^{tr}(\xi) \rangle$, we can write the expression for self-diffusion coefficient in quasi-2D bidisperse ferrofluids:

$$D_{q2D, bi}^{tr} = \left(\frac{\rho_s}{s_s} + \frac{\rho_l}{s_l} \right)^{-1} \left(\sum_{n+m=1}^{\infty} \sum_{i=1}^{XIX} [K(i, n, m)g(i, n, m) \times \langle M_{q2D, ch}^{tr}(k_i(n, m)) \rangle s_l] + \sum_{n=5}^{\infty} f(n) \langle M_{q2D, r}^{tr}(\xi(n)) \rangle s_l \right). \quad (16)$$

III. COMPUTER SIMULATIONS

In order to verify the developed theoretical approach, we performed coarse-grained molecular dynamics simulations [62,63] using the software package ESPRESSO [64,65].

All simulations are done with NVT ensemble with N being the total number of magnetic particles in the system, V being the volume of the simulation box, and T denoting the constant temperature. Molecular dynamics is based on finding time-dependent (t -dependent) solution of Langevin equations of motion in periodic boundary conditions [63]:

$$M_i \frac{d\vec{v}_i}{dt} = \vec{F}_i - \Gamma_T \vec{v}_i + 2\vec{\xi}_i^T, \quad (17)$$

$$I_i \frac{d\vec{\omega}_i}{dt} = \vec{\tau}_i - \Gamma_R \vec{\omega}_i + 2\vec{\xi}_i^R, \quad (18)$$

where for the i th particle M_i denotes the mass tensor, \vec{v}_i is the translational velocity, \vec{F}_i is the force acting on it, Γ_T stands for the translational friction coefficient, $\vec{\xi}_i^T$ is a stochastic force, I_i is particle inertia tensor, $\vec{\omega}_i$ is the rotational velocity, $\vec{\tau}_i$ is a torque acting on the particle, Γ_R is its rotational friction coefficient, and $\vec{\xi}_i^R$ is a stochastic torque. Both $\vec{\xi}_i^T$ and $\vec{\xi}_i^R$ are modeling the random kicks of the solvent molecules in order to avoid simulating the carrier liquid explicitly. Note that hydrodynamic interactions are not considered here, as we are mainly interested in the qualitative impact of dipolar forces, polydispersity, and geometrical constraints.

Thus, along with systems of dipolar magnetic particles, we also modeled a system consisting of soft spheres (without dipoles). Moreover, in order to reduce the dimension of the parameter space, we fix the total volume (area) fraction of particles, $\varphi = \varphi_s + \varphi_l = (N_s v_s + N_l v_l)/V$ ($\rho = \rho_s + \rho_l = (N_s s_s + N_l s_l)/S$), and we vary the ratio between volume (area) fractions of small, $\varphi_s(\rho_s)$, and large, $\varphi_l(\rho_l)$, particles. Simulating bidisperse systems requires us to have a sufficient amount of particles in each fraction, N_s and N_l . We set that the minimal number of particles of each fraction should not be less than 100 for any volume φ and area ρ fractions of interest. Also, it should be noted that we consider 512 magnetic particles as minimum for each system (for monodisperse systems $N = N_s = N_l = 512$).

Long-range magnetic dipole-dipole interaction (2) between all the particles in the dipolar systems are calculated using *dipolar P³M* (*dP³M*) algorithm [66]. In the case of quasi-2D geometry, for speeding up the calculations, full 3D periodicity is assigned to the system, but the interactions in the direction perpendicular to the layer surface are removed with the help of dipolar layer correction method [67].

All the parameters in the simulations are dimensionless. So, all the distances r^* in the computer simulations are measured in units of small particle diameter $\sigma_s = 1$, a magnetic moment square $(m_i^*)^2$ is measured in units of the ratio of a well depth of the potential (3) to the particle diameter cube ε/σ_i^3 . Units of the ratio of the potential well depth to the Boltzmann constant ε/k_B is used to measure the temperature T^* and time t^* is measured in units of square root of the ratio of a particle mass M_i^{part} and particle diameter square to the potential well depth $\sqrt{M_i^{\text{part}} \sigma_i^2 / \varepsilon}$:

$$r^* = \frac{r}{\sigma_s}, \quad (m_i^*)^2 = \frac{m^2}{\varepsilon/\sigma_i^3},$$

$$T^* = \frac{k_B T}{\varepsilon}, \quad t^* = t \sqrt{\frac{\varepsilon}{M_i^{\text{part}} \sigma_i^2}}.$$

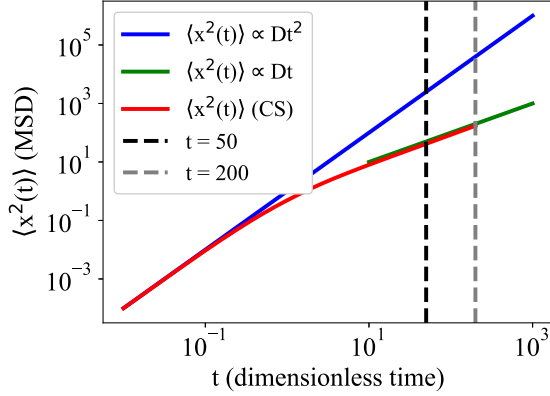


FIG. 2. The mean squared displacement $\langle x^2(t) \rangle$ vs simulation dimensionless time t in a log-log scale. Red curve is the mean squared displacement obtained in simulations for a monodisperse bulk system with particle volume fraction 5% and $\lambda = 3$. Blue curve shows the ballistic part of the curve [$\langle x^2(t) \rangle \propto t^2$]. Green line allows to us see where the diffusive regime is reached [$\langle x^2(t) \rangle \propto t$]. Black and green vertical dashed lines correspond to time moments $t = 50$ and $t = 200$, respectively.

All the computer simulations are performed for the following values of the parameters: $T^* = 1$, $M_i^{\text{part}} = 1$, $I_i = 1$, $\Gamma_T = 1$, and $\Gamma_R = 3/4$. The time step was chosen to be 5×10^{-3} .

We have performed 2×10^5 integrations to reach the thermodynamical equilibrium of the system. The statistical data for further calculations is obtained by the following 2.8×10^6 integrations. Using the statistical data and the algorithm *correlation* [68] in ESPRESSO we calculate the mean squared displacements of all the coordinates of all the particles in different moments of time. For each time moment, we find the value of the mean squared displacement, $\langle x^2(t) \rangle$, given by the expression (1). After that, we can obtain the self-diffusion coefficient as a function of time.

In Fig. 2, we show $\langle x^2(t) \rangle$ as a function of dimensionless simulation time in a log-log scale for a monodisperse bulk system with particle volume fraction 5% and $\lambda = 3$. As one can see, the initial part of the red curve corresponds to the ballistic regime and the mean squared displacement is quadratic with t . The green line shows when the diffusive regime is established and the mean square displacement becomes linear. In molecular dynamics simulations, we obtain the mean squared displacement curve for dimensionless time $t \in [0, 200]$ and found that the segment $t \in [50, 200]$ can be used to calculate the self-diffusion coefficient for all systems. In Fig. 2, this part of the red curve is located between two vertical lines $t = 50$ (black dashed one) and $t = 200$ (green dashed one).

In order to obtain the coefficient like (10) or (16), we perform simulations for both dipolar and nondipolar systems and calculate

$$D^{\text{CS}}(\rho, \lambda) = \frac{D_{\text{dip}}^{\text{CS}}(\rho, \lambda)}{D_0^{\text{CS}}(\rho)}, \quad (19)$$

where $D_{\text{dip}}^{\text{CS}}(\rho, \lambda)$ is the self-diffusion coefficient obtained for systems with dipolar interactions and $D_0^{\text{CS}}(\rho)$ for those without. Considering such a ratio allows us to clearly understand the contribution of dipolar forces to the self-diffusion.

TABLE I. Types of magnetic particles to study different bidisperse systems.

Particle type		Magnetic dipole-dipole interaction parameter (λ_{ll} or λ_{ss})
Large particles	A	3.5
	B	4
Small particles	C	1
	D	1.5
	E	2

IV. RESULTS AND DISCUSSION

We consider two types of large and three types of small magnetic particles. Combining each type of large particles with each type of small ones, we obtain six different bidisperse systems. Particle parameters are provided in Table I.

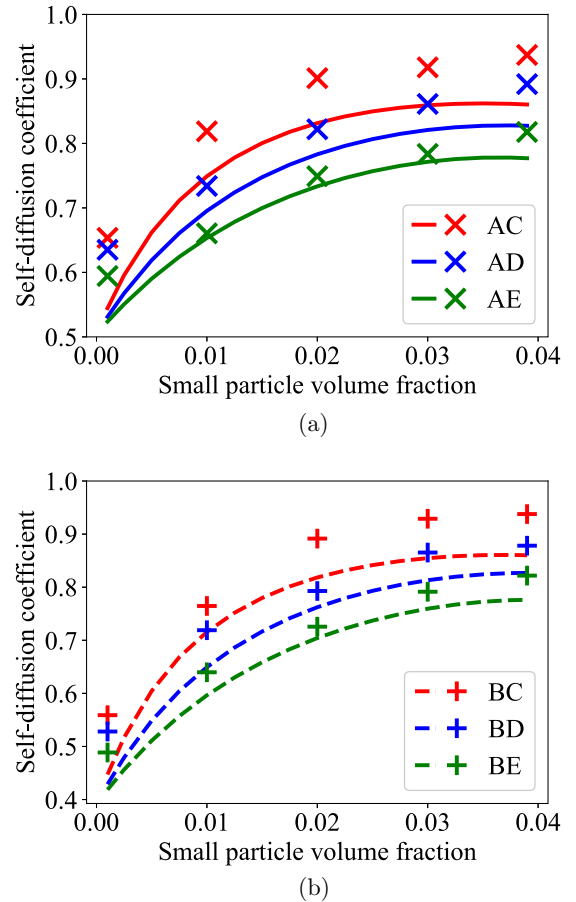
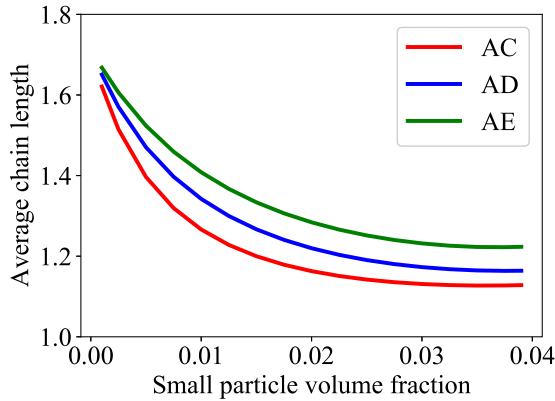
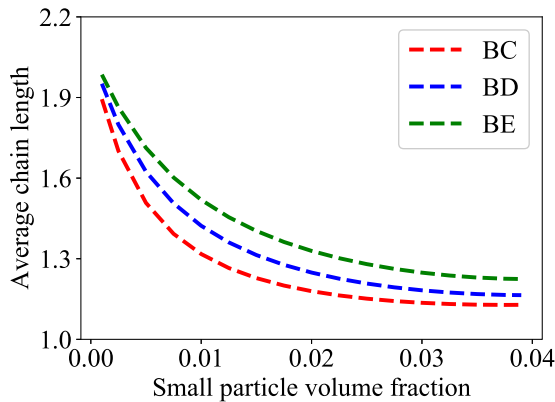


FIG. 3. Self-diffusion coefficient as a function of a small particle volume fraction for ferrofluids in a bulk. Lines are the theoretical results of Eq. (10); symbols are the computer simulation data. Solid lines and \times symbols correspond to systems with large particles of type A, while dotted lines and $+$ symbols correspond to systems with large particles B. Red color is chosen for systems with small particles of type C, blue for systems with small particles D, and green for systems with small particles E.



(a)



(b)

FIG. 4. The dependence of an average chain length on a small particle volume fraction for three-dimensional obtained analytically. Solid lines correspond to systems with large particles of type A, and dotted lines correspond to systems with large particles B. Red color is chosen for systems with small particles of type C, blue for systems with small particles D, and green for systems with small particles E.

A. Bulk systems

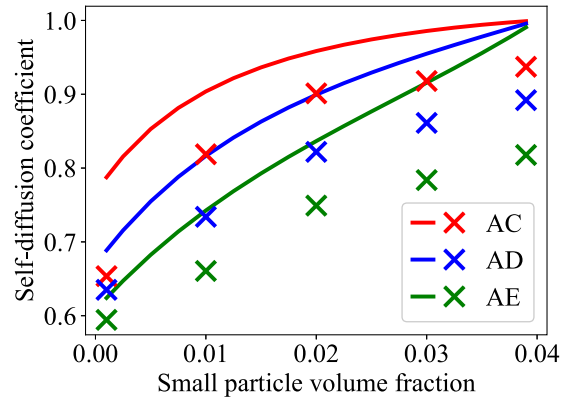
In bulk, we study bidisperse ferrofluids with the total volume fraction $\varphi = 0.04$, and thus starting from a large particle monodisperse system we come to a small particle monodisperse system through a series of binary mixtures with different granulometric compositions.

In Fig. 3, we plot the dependence of the self-diffusion coefficient on a small particle volume fraction for different three-dimensional bidisperse ferrofluids. The self-diffusion coefficient is growing with an increasing small particle volume fraction. This behavior is caused by the chain shortening illustrated in Fig. 4, where the average chain length $L_{ch, 3D}^{av}$,

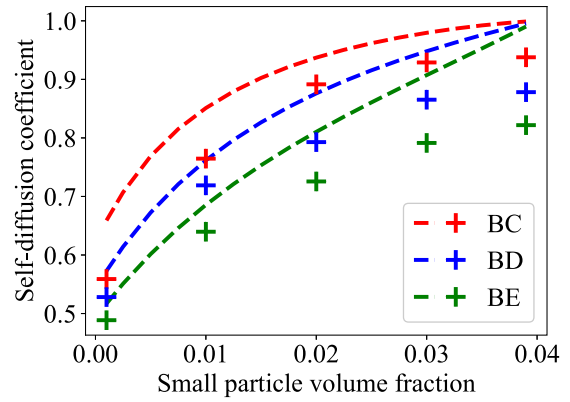
$$L_{ch, 3D}^{av} = \frac{\sum_{n+m=1}^{\infty} \sum_{i=1}^{IV} (n+m)K(i, n, m)g(i, n, m)}{\sum_{n+m=1}^{\infty} \sum_{i=1}^{IV} K(i, n, m)g(i, n, m)}, \quad (20)$$

decreases with growing φ_s . This behavior is usually addressed to as a “poisoning effect” [25]. Shorter chains correlate with faster diffusion.

Figure 3 exhibits good agreement between theory and simulations, especially for the systems with small particles of type E, as the DFT approach described in Sec. II A is known to



(a)

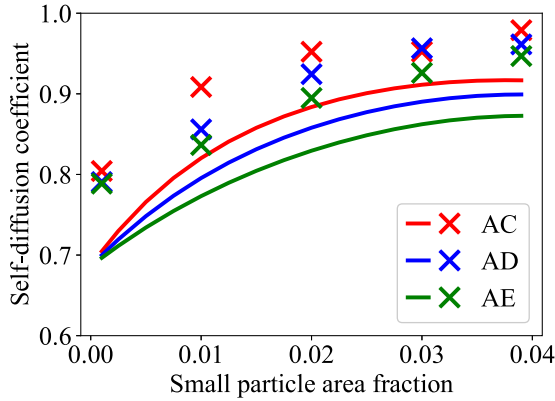


(b)

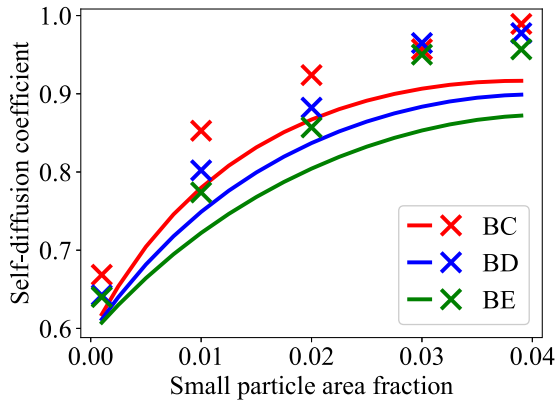
FIG. 5. The self-diffusion coefficient as a function of a small particle volume fraction for three-dimensional magnetic fluids. Same as Fig. 3, but here the lines are the theoretical results obtained from Eq. (10), in which small particles are forced to remain single. Symbols are the computer simulation data. Solid lines and \times symbols correspond to systems with large particles of type A, and dotted lines and $+$ symbols correspond to systems with large particles B. Red color is chosen for systems with small particles of type C, blue for systems with small particles D, and green for systems with small particles E.

overestimate slightly the probability of two weakly interacting particles (like those of types C and D) to form clusters. However, it turns out to be crucial to allow for the possibility of small particles to cluster with each other. The proof can be found in Fig. 5. Here, we plot analytically calculated self-diffusion coefficients for bidisperse systems, restricting small particles to remain nonaggregated. The discrepancy between theoretical results and computer simulation data is clearly large in this case and it grows with φ_s . In fact, more small particles are in the system mean a higher probability of finding small clusters of them that would lead to an overall decrease of the self-diffusion in comparison to small particle ideal gas. In other words, self-diffusion turns out to be very sensitive to even slight changes in granulometry and already a low fraction of small particles that aggregate can manifest itself clearly when studying this quantity.

It is worth noting here that in monodisperse bulk systems of magnetic nanoparticles, the self-diffusion coefficient actually monotonically decreases with increasing particle volume



(a)



(b)

FIG. 6. The dependence of the self-diffusion coefficient on a small particle area fraction for quasi-2D magnetic fluids. Lines are the theoretical results, and symbols are the computer simulation data. Solid lines and \times symbols correspond to systems with large particles of type A, and dotted lines and $+$ symbols correspond to systems with large particles B. Red color is chosen for the systems with small particles of type C, blue for the systems with small particles of type D, and green one for the systems with small particles E.

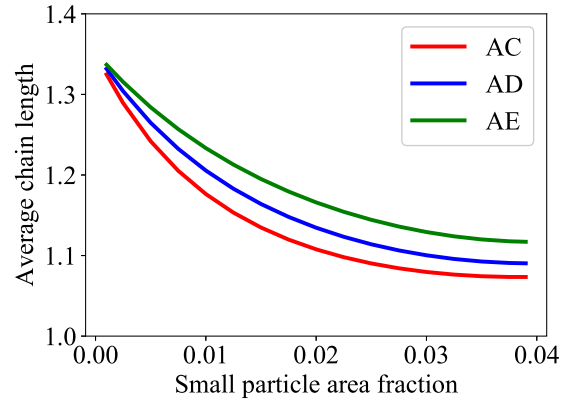
fraction due to the strengthening of interparticle correlations and enhanced cluster formation [69]. So, if we consider two systems with the same volume fraction of magnetic material, but one containing few large particles and another containing both a greater number of particles, including both large and small particles, we can predict that the self-diffusion in the latter will be higher than in its monodisperse counterpart.

B. Quasi-2D layers

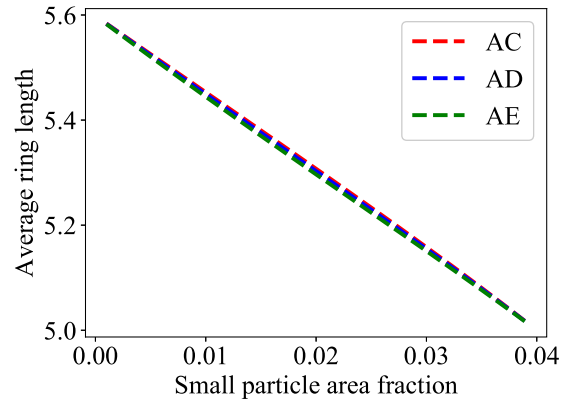
The next step is to investigate whether or not the transition from three-dimensional geometry to a monolayer leads to qualitative changes in self-diffusion behavior of bidisperse ferrofluids. Like in a three-dimensional case described above, in quasi-2D, we study the systems at constant area fraction $\rho = \rho_s + \rho_l = 0.04$.

Similarly to bulk systems, we can define the average chain length for a quasi-2D system:

$$L_{ch, q2D}^{av} = \frac{\sum_{n+m=1}^{\infty} \sum_{i=1}^{XIX} (n+m)K(i, n, m)g(i, n, m)}{\sum_{n+m=1}^{\infty} \sum_{i=1}^{XIX} K(i, n, m)g(i, n, m)}. \quad (21)$$



(a)



(b)

FIG. 7. Average chain and ring lengths as functions of small particle area fraction for quasi-two-dimensional magnetic fluids with large magnetic particles of type A. Solid lines are chosen for average chain lengths, and dotted lines correspond to average ring lengths. Red color is chosen for the system AC, blue for the system AD, and green for the system AE.

The comparison between average chain lengths from the mathematical model and computer simulations can be found in Ref. [58]. Additionally, the average ring length can be calculated as

$$L_{r, q2D}^{av} = \frac{\sum_{n=5}^{\infty} n f(n)}{\sum_{n=5}^{\infty} f(n)}. \quad (22)$$

In Fig. 6, the self-diffusion coefficients for various bidisperse systems are plotted. Solid lines are the analytical results [Eq. (11)], and symbols represent the data obtained via molecular dynamics. It can be seen that qualitatively the picture does not change: The self-diffusion is growing with increasing ρ_s . Even the relative decrease of the chain length in quasi-2D systems is very similar to that in bulk, as seen when comparing the results in Figs. 7(a), 4(a), 8(a), and 4(b). However, quantitatively, the difference between the two geometries is rather clear: Clusters in bulk are on average larger. As an outcome, the relative growth of the self-diffusion on growing fraction of small particles in the system is more pronounced in a monolayer. Finally, the ring size shown in Figs. 7(b) and 8(b) is also quickly decreasing with ρ_s , and the rings actually disappear. So, once small particles are added to the

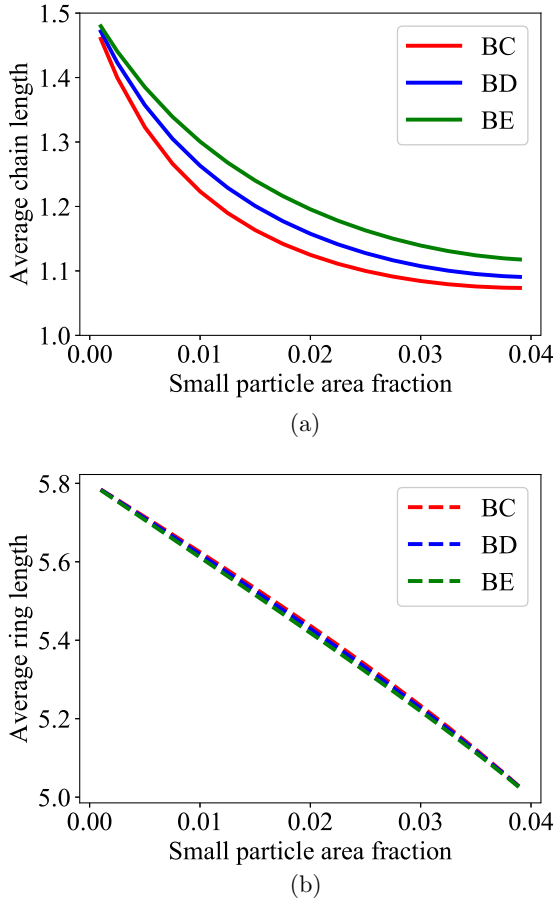


FIG. 8. Average chain and ring lengths as functions of small particle area fraction for quasi-two-dimensional magnetic fluids. Solid lines are chosen for average chain lengths, and dotted lines correspond to average ring lengths. Red color is chosen for the system BC, blue for the system BD, and green for the system BE.

system, the slow contribution of rings to the self-diffusion vanishes.

Besides splitting the system into chains and rings, we can also investigate the contribution of various chain classes to the mobility of the system. In order to do it, we group classes according to the number of small magnetic particles, m , in them. As long as the probability of finding a given cluster goes down with m , we will focus on $m = 1$ and $m = 2$. Chains of classes II and IV contain $m = 1$ small particles, while chains of classes III, V, VI, VIII, and XII contain $m = 2$. Using our theoretical approach, in Fig. 9, we plot self-diffusion coefficients of all the chains consisting of n large and $m = 1$ [see Fig. 9(a)] and $m = 2$ [see Fig. 9(b)] small particles. All curves in the figures have nonmonotonic behavior.

In Fig. 9(a), the red curve corresponds to the chains of the second class and blue one describes the self-diffusion coefficient for chains of the class IV. We can conclude that a contribution of chains of the second class to the self-diffusion is an order of magnitude higher than that of chains of the fourth class. The self-diffusion coefficients of all chain classes containing n large and two small particles are presented in Fig. 9(b). Red color for a curve is used for the chain class III, blue for chain class V, green for chain class VI, yellow

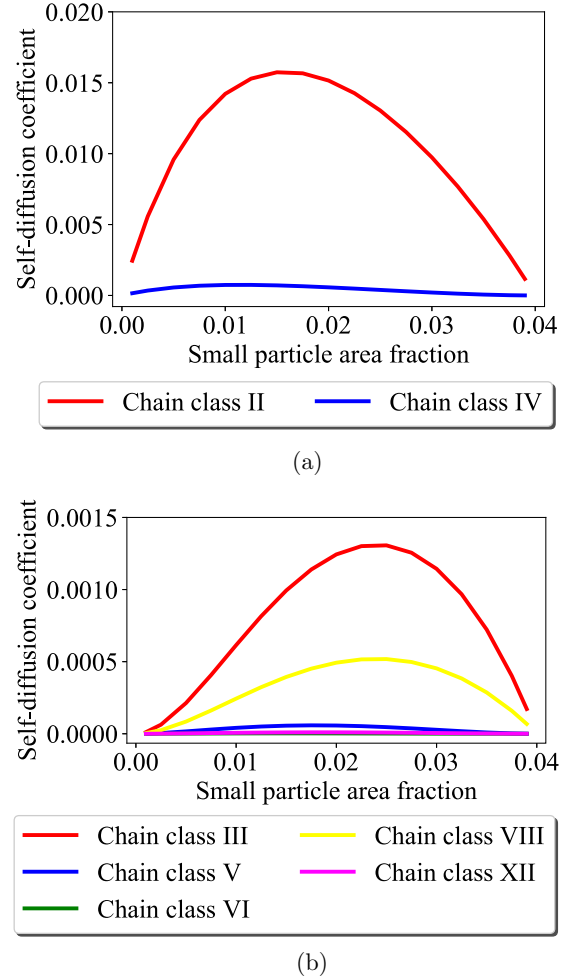


FIG. 9. Self-diffusion coefficients for some classes of chain aggregates: (a) all the chains consisting of n large and one small magnetic particles; (b) all the chains consisting of n large and two small magnetic particles.

for chain class VIII, and magenta for chain class XII. We can highlight contributions of classes III and VIII to the self-diffusion. Chain classes V, VI, and XII have less pronounced contribution. Nonmonotonic behavior of all curves can be explained by the fact that the in both monodisperse limited cases, none of the plotted chain classes can be formed. The reason for the maximum in Fig. 9(a) to be on the left in comparison to that in Fig. 9(b) is the difference in the number of small particles: To form classes with more small particles, one needs a higher small-particle concentration. It is worth mentioning that even though all those chain classes for a given length will be approximated by identical ellipsoids with Eq. (14), the contribution to the average mobility in the system will differ drastically through the chain formation probabilities.

V. CONCLUSIONS

In this work, we put forward an analytical approach to calculate self-diffusion coefficients in bidisperse systems of self-assembling magnetic nanoparticles. This approach is based on the density functional theory that can be applied to describe thermodynamically equilibrium microstructure of

these systems both in bulk and in quasi-2D layers. Another component of the theoretical approach is the approximation of typical clusters by shapes with known mobility. Here, we use ellipsoids and tori to approximate chains and rings respectively. These approximations can be justified in case of relatively short chains and small, not too flexible rings. These conditions are fulfilled either in bulk systems where the interactions between large particles are three to four times stronger than the thermal fluctuations or for the same systems in thin layers, where under the same conditions along with chains, also rings of five to seven nanoparticles form. The analytical model proposed here does not take into account hydrodynamic interparticle interactions and is meant to analyze the impact of cluster formation and polydispersity on the self-diffusion. Thus, in order to verify such a theoretical approach, we performed hydrodynamics-free molecular dynamics simulations.

We find that, on the one hand, the proposed analytical approach is reliable in the discussed parameter range, namely volume or area fraction of magnetic material below or around 5%, magnetic interactions between the particles are up to four times higher than $k_B T$; on the other hand, we show that in case the total volume or area fraction of magnetic material is fixed in the system, one can increase self-diffusion by

considering mixtures of small and large particles, where the clusters are smaller and as such the overall diffusion is faster. This effect is more pronounced in quasi-2D layers, where the clusters are in general smaller and with growing small particle fraction the size and the number of slow ring-like aggregates decays rapidly and the rings basically disappear. Finally, we discover that even a low fraction of small particles that is forming chains in the systems—their interactions are barely higher than the thermal fluctuations—manifests itself in the self-diffusion behavior, unlike, for instance in scattering or magnetic properties previously investigated [25,51]. We show it by confronting simulation results and analytical predictions with different number of structural units taken into account.

This work forms a solid basis for investigating gradient diffusion as well as the effects of hydrodynamics on the diffusion in magnetic nanoparticle systems.

ACKNOWLEDGMENTS

This research has been supported by the Russian Science Foundation Grant No. 19-72-10033. Computer simulations have been performed in UrFU Cluster and Vienna Scientific Cluster (VSC3).

-
- [1] R. Rosensweig, *Ferrohydrodynamics* (Cambridge University Press, New York, 1985).
 - [2] E. L. Resler and R. Rosensweig, Magnetocaloric power, *AIAA J.* **2**, 1418 (1964).
 - [3] E. Y. Blums, M. M. Mayorov, and A. O. Cebers, *Magnetic Fluids* (Walter de Gruyter, Berlin, 1997).
 - [4] I. Anton, I. de Sabata, and L. Vékás, Application orientated researches on magnetic fluids, *J. Magn. Magn. Mater.* **85**, 219 (1990).
 - [5] A. S. Lübke, C. Alexiou, and C. Bergmann, Clinical applications of magnetic drug targeting, *J. Surg. Res.* **95**, 200 (2001).
 - [6] A. Zubarev, L. Iskakova, and A. Abu-Bakr, Magnetic hyperthermia in solid magnetic colloids, *Physica A (Amsterdam, Neth.)* **467**, 59 (2017).
 - [7] A. Yu. Zubarev, Magnetic hyperthermia in a system of ferromagnetic particles, frozen in a carrier medium: Effect of interparticle interactions, *Phys. Rev. E* **98**, 032610 (2018).
 - [8] S.-J. Lee, J.-R. Jeong, S.-C. Shin, J.-C. Kim, Y.-H. Chang, Y.-M. Chang, and J.-D.-D. Kim, Nanoparticles of magnetic ferric oxides encapsulated with poly(*d, l* lactide-co-glycolide) and their applications to magnetic resonance imaging contrast agent, *J. Magn. Magn. Mater.* **272**, 2432 (2004).
 - [9] A. Yu. Zubarev, Magnetic hyperthermia in a system of immobilized magnetically interacting particles, *Phys. Rev. E* **99**, 062609 (2019).
 - [10] B. Y. Ku, M.-L. Chan, Z. Ma, and D. A. Horsley, Frequency-domain birefringence measurement of biological binding to magnetic nanoparticles, *J. Magn. Magn. Mater.* **320**, 2279 (2008).
 - [11] A. Abu-Bakr and A. Zubarev, Effect of interparticle interaction on magnetic hyperthermia: Homogeneous spatial distribution of the particles, *Phil. Trans. R. Soc. A* **377**, 20180216 (2019).
 - [12] P. Licinio, A. Teixeira, G. Safar, M. Andrade, L. Meira-Belo, and U. Leitão, Diffusion-limited aggregation of magnetic particles under a field, *J. Magn. Magn. Mater.* **226–230**, 1945 (2001).
 - [13] J.-C. Bacri, A. Cebers, A. Bourdon, G. Demouchy, B. M. Heegaard, B. Kashevsky, and R. Perzynski, Transient grating in a ferrofluid under magnetic field: Effect of magnetic interactions on the diffusion coefficient of translation, *Phys. Rev. E* **52**, 3936 (1995).
 - [14] A. Mertelj, L. Cmok, and M. Čopič, Anomalous diffusion in ferrofluids, *Phys. Rev. E* **79**, 041402 (2009).
 - [15] G. K. Batchelor, Brownian diffusion of particles with hydrodynamic interaction, *J. Fluid Mech.* **74**, 1 (1976).
 - [16] B. Cichoki and B. U. Felderhof, Sedimentation and self-diffusion in suspensions of spherical particles, *Physica A (Amsterdam, Neth.)* **154**, 213 (1989).
 - [17] K. I. Morozov, Gradient diffusion in concentrated ferrocolloids under the influence of a magnetic field, *Phys. Rev. E* **53**, 3841 (1996).
 - [18] P. Ilg, Anisotropic diffusion in nematic liquid crystals and in ferrofluids, *Phys. Rev. E* **71**, 051407 (2005).
 - [19] A. F. Pshenichnikov, E. A. Elfimova, and A. O. Ivanov, Magnetophoresis, sedimentation, and diffusion of particles in concentrated magnetic fluids, *J. Chem. Phys.* **134**, 184508 (2011).
 - [20] A. Y. Zubarev, On the theory of transport phenomena in ferrofluids. effect of chain-like aggregates, *Physica A (Amsterdam, Neth.)* **392**, 72 (2013).
 - [21] J. Jordanovic, S. Jager, and S. H. L. Klapp, Crossover from Normal to Anomalous Diffusion in Systems of Field-Aligned Dipolar Particles, *Phys. Rev. Lett.* **106**, 038301 (2011).

- [22] S. Fedotov, A. Tan, and A. Zubarev, Persistent random walk of cells involving anomalous effects and random death, *Phys. Rev. E* **91**, 042124 (2015).
- [23] M. Hod, A. Dobroserdova, S. Samin, C. Dobbrow, A. Schmidt, M. Gottlieb, and S. Kantorovich, Dilution effects on combined magnetic and electric dipole interactions: A study of ferromagnetic cobalt nanoparticles with tuneable interactions, *J. Chem. Phys.* **147**, 084901 (2017).
- [24] S. Kantorovich, Chain aggregate structure in polydisperse ferrofluids: Different applications, *J. Magn. Magn. Mater.* **289**, 203 (2005).
- [25] A. O. Ivanov and S. S. Kantorovich, Chain aggregate structure and magnetic birefringence in polydisperse ferrofluids, *Phys. Rev. E* **70**, 021401 (2004).
- [26] S. Kantorovich and A. Ivanov, Formation of chain aggregates in magnetic fluids: An influence of polydispersity, *J. Magn. Magn. Mater.* **252**, 244 (2002).
- [27] C. Holm, A. Ivanov, S. Kantorovich, and E. Pyanzina, Polydispersity influence upon magnetic properties of aggregated ferrofluids, *Z. Phys. Chem.* **220**, 105 (2006).
- [28] N. Daffé, J. Zečević, K. Trohidou, M. Sikora, M. Rovezzi, C. Carvallo, M. Vasilakaki, S. Neveu, J. Meeldijk, N. Bouldi, V. Gavrilov, Y. Guyodo, F. Choueikani, V. Dupuis, D. Taverna, P. Saintavit, and A. Juhin, Bad neighbour, good neighbour: How magnetic dipole interactions between soft and hard ferrimagnetic nanoparticles affect macroscopic magnetic properties in ferrofluids, *Nanoscale* **12**, 11222 (2020).
- [29] J. Cerdà, S. Kantorovich, and C. Holm, Aggregate formation in ferrofluid monolayers: Simulations and theory, *J. Phys.: Condens. Matter* **20**, 204125 (2008).
- [30] T. A. Prokopieva, V. A. Danilov, S. S. Kantorovich, and C. Holm, Ground state structures in ferrofluid monolayers, *Phys. Rev. E* **80**, 031404 (2009).
- [31] T. Prokopieva, V. Danilov, A. Dobroserdova, S. Kantorovich, and C. Holm, Ground state structures in ferrofluid monolayers, *J. Magn. Magn. Mater.* **323**, 1298 (2011).
- [32] T. Prokopieva, V. Danilov, and S. Kantorovich, Ground state microstructure of a ferrofluid thin layer, *J. Exp. Theor. Phys.* **113**, 435 (2011).
- [33] S. Kantorovich, J. Cerdà, and C. Holm, Microstructure analysis of monodisperse ferrofluid monolayers: Theory and simulation, *Phys. Chem. Chem. Phys.* **10**, 1883 (2008).
- [34] J.-J. Weis, Simulation of quasi-two-dimensional dipolar systems, *J. Phys.: Condens. Matter* **15**, S1471 (2003).
- [35] J. Weis, J. Tavares, and M. Telo Da Gama, Structural and conformational properties of a quasi-two-dimensional dipolar fluid, *J. Phys.: Condens. Matter* **14**, 9171 (2002).
- [36] M. Klokkenburg, R. Dullens, W. Kegels, B. Ern , and A. Philipse, Quantitative Real-Space Analysis of Self-Assembled Structures of Magnetic Dipolar Colloids, *Phys. Rev. Lett.* **96**, 037203 (2006).
- [37] K. Butter, P. Bomans, P. Frederik, G. Vroege, and A. Philipse, Direct observation of dipolar chains in ferrofluids in zero field using cryogenic electron microscopy, *J. Phys.: Condens. Matter* **15**, S1451 (2003).
- [38] P. Duncan and P. Camp, Structure and dynamics in a monolayer of dipolar spheres, *J. Chem. Phys.* **121**, 11322 (2004).
- [39] E. Lomba, F. Lado, and J. J. Weis, Structure and thermodynamics of a ferrofluid monolayer, *Phys. Rev. E* **61**, 3838 (2000).
- [40] A. Ghazali and J.-C. L vy, Two-dimensional arrangements of magnetic nanoparticles, *Phys. Rev. B: Condens. Matter Mater. Phys.* **67**, 064409 (2003).
- [41] W. Wen, F. Kun, K. F. P l, D. W. Zheng, and K. N. Tu, Aggregation kinetics and stability of structures formed by magnetic microspheres, *Phys. Rev. E* **59**, R4758(R) (1999).
- [42] E. Purcell, *Electricity and Magnetism: Berkeley Physics Course* (Nauka, Moscow, 1983).
- [43] J. D. Weeks, D. Chandler, and H. C. Andersen, Role of repulsive forces in determining the equilibrium structure of simple liquids, *J. Chem. Phys.* **54**, 5237 (1971).
- [44] J. E. Lennard-Jones, On the determination of molecular fields, *Proc. R. Soc. London A* **106**, 441 (1924).
- [45] L. Rovigatti, J. Russo, and F. Sciortino, No Evidence of Gas-Liquid Coexistence in Dipolar Hard Spheres, *Phys. Rev. Lett.* **107**, 237801 (2011).
- [46] A. Ivanov, S. Kantorovich, L. Rovigatti, J. Tavares, and F. Sciortino, Low temperature structural transitions in dipolar hard spheres: The influence on magnetic properties, *J. Magn. Magn. Mater.* **383**, 272 (2015).
- [47] L. Rovigatti, S. Kantorovich, A. Ivanov, J. Tavares, and F. Sciortino, Branching Points in the Low-Temperature Dipolar Hard Sphere Fluid, *J. Chem. Phys.* **139**, 134901 (2013).
- [48] A. Elkady, L. Iskakova, and A. Zubarev, On the self-assembly of net-like nanostructures in ferrofluids, *Physica A (Amsterdam, Neth.)* **428**, 257 (2015).
- [49] A. Yu. Zubarev and L. Yu. Iskakova, Theory of physical properties of magnetic liquids with chain aggregates, *J. Exp. Theor. Phys.* **80**, 857 (1995).
- [50] L. Rovigatti, J. M. Tavares, and F. Sciortino, Self-Assembly in Chains, Rings, and Branches: A Single Component System with Two Critical Points, *Phys. Rev. Lett.* **111**, 168302 (2013).
- [51] A. Ivanov, S. Kantorovich, V. Mendelev, and E. Pyanzina, Ferrofluid aggregation in chains under the influence of a magnetic field, *J. Magn. Magn. Mater.* **300**, e206 (2006).
- [52] F. Perrin, Brownian motion of an ellipsoid—I. Dielectric dispersion for ellipsoidal molecules, *J. Phys. Radium* **5**, 497 (1934).
- [53] S. Kim and S. J. Karrila, *Microhydrodynamics: Principles and Selected Applications* (Butterworth-Heinemann, New York, 1991).
- [54] Y. Han, A. M. Alsayed, M. Nobili, J. Zhang, T. C. Lubensky, and A. G. Yodh, Brownian motion of an ellipsoid, *Science* **314**, 626 (2006).
- [55] Y. Han, A. Alsayed, M. Nobili, and A. G. Yodh, Quasi-two-dimensional diffusion of single ellipsoids: Aspect ratio and confinement effects, *Phys. Rev. E* **80**, 011403 (2009).
- [56] M. Hoffmann, C. S. Wagner, L. Harnau, and A. Wittemann, 3d Brownian diffusion of submicron-sized particle clusters, *ACS Nano* **3**, 3326 (2009).
- [57] Z. Zheng and Y. Han, Self-diffusion in two-dimensional hard ellipsoid suspensions, *J. Chem. Phys.* **133**, 124509 (2010).
- [58] E. S. Minina, A. B. Muratova (Dobroserdova), J. J. Cerd , and S. S. Kantorovich, Microstructure of bidisperse ferrofluids in a thin layer, *J. Exp. Theor. Phys.* **116**, 424 (2013).

- [59] A. Dobroserdova, E. Minina, J. J. Cerdà, C. Holm, and S. Kantorovich, Microstructure of bidisperse ferrofluids in a monolayer, *Solid State Phenom.* **190**, 625 (2012).
- [60] R. E. Johnson and T. Y. Wu, Hydromechanics of low-Reynolds-number flow, part 5: Motion of a slender torus, *J. Fluid Mech.* **95**, 263 (1979).
- [61] R. M. Thaokar, Brownian motion of a torus, *Colloids Surf., A: Physicochemical and Engineering Aspects* **317**, 650 (2008).
- [62] M. P. Allen and D. J. Tildesley, *Computer Simulation of Liquids* (Oxford University Press, Oxford, UK, 1989).
- [63] D. Frenkel and B. Smit, *Understanding Molecular Simulation: From Algorithms to Applications* (Academic Press, New York, 2002).
- [64] A. Arnold, O. Lenz, S. Kesselheim, R. Weeber, F. Fahrenberger, D. Roehm, P. Košovan, and C. Holm, ESPResSo 3.1—Molecular dynamics software for coarse-grained models, in *Meshfree Methods for Partial Differential Equations VI*, Lecture Notes in Computational Science and Engineering Vol. 89, edited by M. Griebel and M. A. Schweitzer (Springer, Berlin, 2013), pp. 1–23.
- [65] H. J. Limbach, A. Arnold, B. A. Mann, and C. Holm, Espresso—An extensible simulation package for research on soft matter systems, *Comput. Phys. Commun.* **174**, 704 (2006).
- [66] J. J. Cerdà, V. Ballenegger, O. Lenz, and C. Holm, p^3m algorithm for dipolar interactions, *J. Chem. Phys.* **129**, 234104 (2008).
- [67] A. Arnold, J. de Joannis, and C. Holm, Electrostatics in periodic slab geometries. I, *J. Chem. Phys.* **117**, 2496 (2002).
- [68] A. Arnold, O. Lenz, S. Kesselheim, R. Weeber, F. Fahrenberger, D. Roehm, P. Košovan, and C. Holm, ESPResSo 3.1: Molecular Dynamics Software for Coarse-Grained Models, In: Griebel M., Schweitzer M. (eds), *Meshfree Methods for Partial Differential Equations VI. Lecture Notes in Computational Science and Engineering* vol. 89 (Springer, Berlin, Heidelberg, 2013).
- [69] A. Dobroserdova and S. Kantorovich, Self-diffusion in monodisperse three-dimensional magnetic fluids by molecular dynamics simulations, *J. Magn. Magn. Mater.* **431**, 176 (2017).